J. Math. Biol. (1997) 36: 24–40

Journal of Mathematical Biology

Complex dynamic behaviour of autonomous microbial food chains

B. W. Kooi, M. P. Boer, S. A. L. M. Kooijman

Received 8 November 1995; received in revised form 7 January 1997

Faculty of Biology, Free University, De Boelelaan 1087, 1081 HV Amsterdam, The Netherlands

Abstract. The dynamic behaviour of food chains under chemostat conditions is studied. The microbial food chain consists of substrate (non-growing resources), bacteria (prey), ciliates (predator) and carnivore (top predator). The governing equations are formulated at the population level. Yet these equations are derived from a dynamic energy budget model formulated at the individual level. The resulting model is an autonomous system of four first-order ordinary differential equations. These food chains resemble those occuring in ecosystems. Then the prey is generally assumed to grow logistically. Therefore the model of these systems is formed by three first-order ordinary differential equations. As with these ecosystems, there is chaotic behaviour of the autonomous microbial food chain under chemostat conditions with biologically relevant parameter values. It appears that the trajectories on the attractors consists of two superimposed oscillatory behaviours, a slow one for predator–top predator and a fast one for the prey–predator on one branch at which the top predator increases slowly. In some regions of the parameter space there are multiple attractors.

Key words: Bifurcation diagram – Chaos – Chemostat – Food chain – Existence and stability – Limit cycle

1 Introduction

The Monod model [17] is the classical basis for modelling the dynamics of populations consisting of unicellular organisms. In that model food is ingested with a rate proportional to the Holling type II functional response. A fixed part of the ingested food is used for growth. Nisbet et al. [18] investigated a variant of that model, the Monod-Herbert model [5]. Then ingested food is not only used for growth but also for maintenance while these costs are proportional to the biomass of the population.

Cunningham and Nisbet [3] and Nisbet et al. [18] studied the dynamic behaviour of a bi-trophic microbial food chain consisting of substrate, bacterium and ciliate in a chemostat, a well stirred vessel. They showed that the introduction of maintenance has a stabilizing effect, especially for low dilution rates.

Kot et al. [12] and Pavlou and Kevrekidis [19] studied the complex dynamics of a forced bi-trophic microbial food chain in a chemostat with forcing in the form of a periodic inflow of substrate. In both papers the set of parameter values proposed in [3] were used. The forced system displayed quasiperiodicity, phase locking, periodic doubling and chaotic dynamical behaviour.

In this paper the bi-trophic food chain is extended to a tri-trophic chain with top predator. The substrate supply to the chain is constant rather than oscillatory, so that the system is autonomous. For each trophic level a simplified version of the Dynamic Energy Budget (DEB) model [9, 11], is used. In this individual-based model energy reserves act as a buffer. They impose a kind of inertia on the response to changing food conditions. Also taken into account are maintenance costs. The non-specific DEB model describes species at all trophic levels by the same set of ODEs, only the parameter values differ for different species. We will also use the set of parameter values proposed in [3] for the substrate, prey, predator dynamics and extrapolated values for the top predator. Hence, the parameter settings in this study are relevant for bacteria living on glucose at 25 °C, ciliates such as *Tetrahymena* sp. or *Paramecium* and carnivorous ciliates such as *Didinium nasutum*.

For a bi-trophic food chain the autonomous system exhibits only simple limit sets being equilibria and limit cycles. The transition of an equilibrium to a limit cycle at a Hopf bifurcation with increasing the concentration in the reservoir, may be viewed as an example of the paradox of enrichment (Roosenzweig [21]). We will show that the situation for a tri-trophic food chain differs significantly. In some region of the parameter space the introduction of the top predator in an oscillating bi-trophic food chain can stabilize the system to a positive equilibrium. The system can also converge to a positive limit cycle, or chaotic behaviour can be the result. In another region of the parameter space the top predator can not invade the system.

The proposed model resembles that for ecosystems, consisting of a tri-trophic food chain (prey, predator and top predator) with logistic prey, studied intensively in the literature, see for instance [4, 7, 8, 14, 16]. In the chemostat model the substrate, which is taken to be inert, is modelled explicitly.

The autonomous tri-trophic food chain with logistic prey exhibits chaotic dynamics in long-term behaviour when reasonable parameter values are chosen, as shown in [4, 14]. The occurrence of chaotic behaviour proved to be very sensitive to the choice of the relative death rates of the populations at the three trophic levels. In this paper we will obtain chaotic behaviour, not by tuning parameters of the populations but by tuning the chemostat control parameters: the dilution rate and the concentration in the reservoir.

We will present one- and two-parameter bifurcation diagrams. The two-parameter bifurcation diagrams (in the microbial literature often called 'operating diagrams') are useful to examine the complex dynamics. These diagrams show the asymptotic behaviour, existence of positive equilibria, as well as limit cycles and their stability as a function of the two control parameters. A continuation technique is used to calculate the bifurcation curves in the parameter space, such as transcritical, tangent, Hopf and flip bifurcations of equilibria and limit cycles. To calculate most of these bifurcation curves, we used LOCBIF [6, 13], an interactive software package implementing a continuation technique in conjunction with detection of high codimension bifurcation points.

We will also give one-parameter bifurcation diagrams with the long-term maximum values for the biomass of the top predator as function of one control parameter, the dilution rate. The results given in the one-parameter bifurcation diagrams show that there is chaotic behaviour of the autonomous system in a biologically interesting region of the parameter space. On top of these one-parameter diagrams the associated two-parameter diagram is plotted. This facilitates the analysis of the routes to chaotic behaviour.

The chaotic attractor lies in the surface of a "teacup", see Fig. 1. In the handle the top predator diminishes whereas the prey and predator are nearly

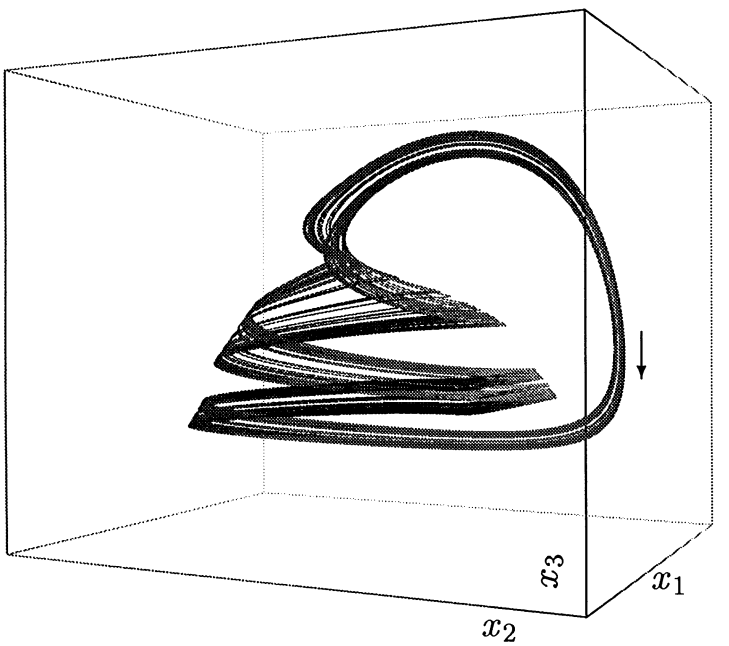

Fig. 1. Phase portrait for dilution rate $D = 0.03\,\mathrm{h}^{-1}$ and concentration in the reservoir $x_r = 292.5\,\mathrm{mg\,dm}^{-3}$. The ranges for the three variables are $0 \leqq x_1 \leqq 100\,\mathrm{mg\,dm}^{-3}$, $0 \leqq x_2 \leqq 30\,\mathrm{mg\,dm}^{-3}$ and $0 \leqq x_3 \leqq 6\,\mathrm{mg\,dm}^{-3}$. The chaotic attractor traces the surface of a "teacup"

constant. Then, starting over the rim, the prey-predator oscillate while the top predator increases relatively slowly giving a trajectory on the cup which enters in the handle again.

2 The model

Let $x_0(t)$ denote density of the resource (substrate). Furthermore, let $x_i(t)$, $i = 1, 2, 3$ denote biomass densities of prey, predator and top predator, respectively, and $e_i(t)$, $i = 1, 2, 3$ denote scaled reserve densities. The DEB model reads

$$\frac{dx_0}{dt} = (x_r - x_0)D - I_{0,1}f_{0,1}x_1\,, \tag{1}$$

$$\frac{dx_i}{dt} = x_i\frac{v_{i-1,i}e_i - m_i g_i}{e_i + g_i} - Dx_i - I_{i,i+1}f_{i,i+1}x_{i+1}, \quad \text{for } i = 1, 2\,, \tag{2}$$

$$\frac{dx_3}{dt} = x_3\frac{v_{2,3}e_3 - m_3 g_3}{e_3 + g_3} - Dx_3\,, \tag{3}$$

$$\frac{de_i}{dt} = v_{i-1,i}(f_{i-1,i} - e_i), \quad \text{for } i = 1, 2, 3\,, \tag{4}$$

where $f_{i-1,i} = x_{i-1}/(k_{i-1,i} + x_{i-1})$ is the scaled Holling type II functional response. The first term on the right hand-sides of Eqs. (2) and (3) is the growth term of the population whereby we assume that food uptake is proportional to biomass density. The term $v_{i-1,i}e_i$ is the assimilation rate and the term $m_i g_i$ is associated with the energetic costs for maintenance, also proportional to the biomass density x_i. The term in the denominator is the sum of the energetic costs g_i for growth plus an extra term, the energy reserves e_i. Energy reserves e_i is the energy density divided by the maximum energy density which is assumed to be a fixed parameter. For a complete description of the model and the biological meaning of the parameters the reader is referred to [11] and also Table 1.

In this paper, as in [9], we assume that the reserve densities are in quasi-steady state and $e_i(t) = f_{i-1,i}(t)$. The simplified DEB model now reads

$$\frac{dx_0}{dt} = (x_r - x_0)\,D - I_{0,1}f_{0,1}x_1\,, \tag{5}$$

$$\frac{dx_1}{dt} = x_1\frac{v_{0,1}f_{0,1} - m_1 g_1}{f_{0,1} + g_1} - Dx_1 - I_{1,2}f_{1,2}x_2\,, \tag{6}$$

$$\frac{dx_2}{dt} = x_2\frac{v_{1,2}f_{1,2} - m_2 g_2}{f_{1,2} + g_2} - Dx_2 - I_{2,3}f_{2,3}x_3\,, \tag{7}$$

$$\frac{dx_3}{dt} = x_3\frac{v_{2,3}f_{2,3} - m_3 g_3}{f_{2,3} + g_3} - Dx_3\,. \tag{8}$$

Table 1. Parameters and state variables; t = time, m = biomass, v = volume of the reactor. The subindex denotes the trophic level, $i = 0$ substrate, $i = 1$ bacteria, $i = 2$ ciliate and $i = 3$ carnivore

Parameter	Dimension	Units	Interpretation
t	t	h	Time
x_0	$\mathrm{m\,v^{-1}}$	$\mathrm{mg\,dm^{-3}}$	Substrate density
x_i	$\mathrm{m\,v^{-1}}$	$\mathrm{mg\,dm^{-3}}$	Biomass density
x_r	$\mathrm{m\,v^{-1}}$	$\mathrm{mg\,dm^{-3}}$	Substrate concentration in reservoir
D	$\mathrm{t^{-1}}$	$\mathrm{h^{-1}}$	Dilution rate
$f_{i-1,i}$	–	–	Functional response
$k_{i-1,i}$	$\mathrm{m\,v^{-1}}$	$\mathrm{mg\,dm^{-3}}$	Saturation constant
$I_{i-1,i}$	$\mathrm{t^{-1}}$	$\mathrm{h^{-1}}$	Maximum food uptake rate
$\mu_{i-1,i}$	$\mathrm{t^{-1}}$	$\mathrm{h^{-1}}$	Overall population growth rate
$y_{i-1,i}$	–	–	Yield
m_i	$\mathrm{t^{-1}}$	$\mathrm{h^{-1}}$	Maintenance rate coefficient
$v_{i-1,i}$	$\mathrm{t^{-1}}$	$\mathrm{h^{-1}}$	Energy conductance, $\propto$ assimilation rate
g_i	–	–	Energy investment ratio, $\propto$ costs for growth

Table 2. Parameter set for bacterium-ciliate models, after Cunningham & Nisbet [3] and [18]. The values for the new parameters m_i (equal to 5% of maximum growth rate $\mu_{i-1,i}$) and g_i are also given. The relationships $I_{i-1,i} = \mu_{i-1,i}/y_{i-1,i}$ and $v_{i-1,i} = \mu_{i-1,i}g_i$ hold true for $i = 1, 2, 3$. The ranges for the control parameters are $0 < D < \mu_{0,1}$ and $0 < x_r \leqq 300\ \mathrm{mg\,dm^{-3}}$

Parameter	Unit	Values		
		$i = 1$	$i = 2$	$i = 3$
$y_{i-1,i}$	–	0.4	0.6	0.6
$\mu_{i-1,i}$	$\mathrm{h^{-1}}$	0.5	0.2	0.15
$k_{i-1,i}$	$\mathrm{mg\,dm^{-3}}$	8	9	10
$I_{i-1,i}$	$\mathrm{h^{-1}}$	1.25	0.33	0.25
m_i	$\mathrm{h^{-1}}$	0.025	0.01	0.0075
g_i	–	80.0	1.0	0.504
$v_{i-1,i}$	$\mathrm{h^{-1}}$	40.0	0.2	0.0756

The chemostat parameters for the model are presented in Table 2. The values for $i = 1, 2$ (prey, predator) are given in Cunningham and Nisbet [3] and are based on measured bacterium and ciliate cultures in the chemostat. This set of parameter values with $m_i = 0$ was also used in [12, 19] for the study of the complex dynamics of a forced microbial food chain. In our study the maintenance coefficient m_i is chosen to be 5% of the maximum growth rate $\mu_{i-1,i}$. The values for $i = 3$ (top predator) are extrapolated from those given in [3], those of the parameter g_i are not based on experimental data but they are in a reasonable range for species such as *Didinium nasutum*, as shown in [10].

3 Equilibria and period-1 limit cycles

The bifurcation parameters are D and x_r. The range of the parameter x_r, the substrate density in the reservoir, is taken $0 < x_r \leqq 300\,\mathrm{mg\,dm^{-3}}$, while for the dilution rate D, we study the meaningful range $0 < D < \mu_{0,1}$. An analytical evaluation of the normal form in specific equilibrium points, as performed in [7, 8, 14] for ecosystem models, is impossible. One has to resort to numerical approximation.

In Fig. 2 we give the two-parameter bifurcation diagram for the food chain of substrate (x_0), bacteria (x_1), ciliates (x_2) and carnivore (x_3), described by system (5)–(8). The results are based upon stability analysis of the positive equilibria and limit cycles. In this diagram the region with washout of the predator and top predator is to the left of the curve labelled $TC_{e,2}$. In this region x_2 and x_3 are zero in equilibrium. Only present in the chemostat are the bacteria (prey), $x_1 > 0$, and their food, the substrate $0 < x_0 < x_r$. The equilibria are stable. At the left of the curve $TC_{e,1}$ there is total washout of all biomass, that is, only substrate is present in the reactor with concentration equal to that in the reservoir, $x_0 = x_r$.

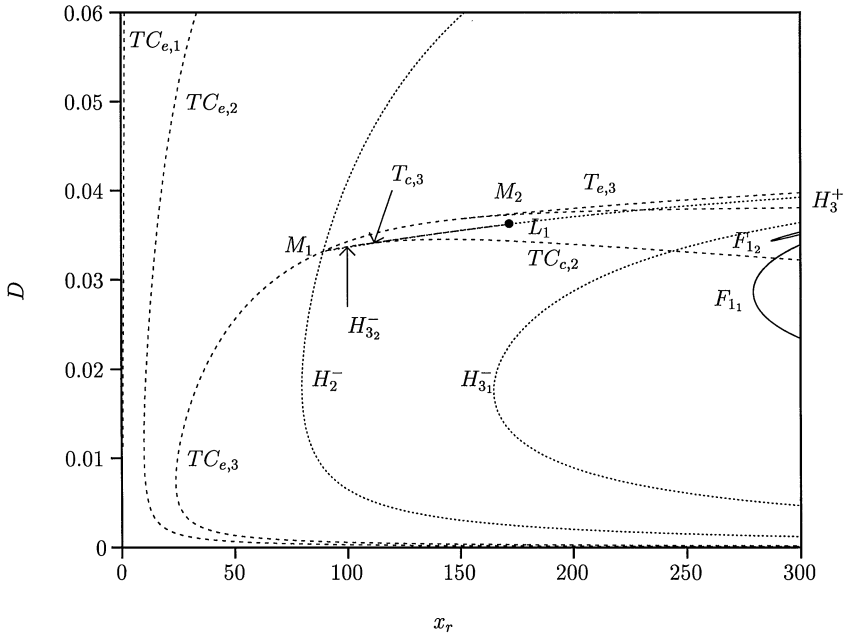

Fig. 2. Two-parameter bifurcation diagram for tri-trophic food chain in chemostat situation (Eqs. 5, 6, 7, 8). Values assigned to physiological parameters are listed in Table 2. Dotted curves H_2^-, H_3^+, $H_{3_2}^-$ and $H_{3_1}^-$ mark Hopf bifurcations, curves $TC_{e,1}$, $TC_{e,2}$, $TC_{e,3}$ mark transcritical bifurcations while $T_{e,3}$ marks a tangent bifurcation curve and curve $TC_{c,2}$ marks a transcritical bifurcation for limit cycles with $x_3 = 0$. Point M_1 is intersection point for bifurcation curves, $TC_{e,3}$, H_2^-, $H_{3_2}^-$, $TC_{c,2}$ point and point M_2 is intersection point for bifurcation curves, $TC_{e,3}$, $T_{e,3}$, respectively

On the left of the Hopf bifurcation curve H_2^- there is stable coexistence of bacteria and ciliates (prey and predator). The three curves mentioned before, $TC_{e,1}$, $TC_{e,2}$ and H_2^-, are for the bi-trophic food chain and were already presented in Nisbet et al. [18]. In the region on the right of the Hopf bifurcation curve H_2^- there is unstable coexistence of both species and there exist stable limit cycles with $x_3 = 0$ beyond the curve $TC_{c,2}$ and unstable limit cycles below this curve. In the latter case the system will finally converge to a positive attractor when a small amount of top predator is introduced in the cycling food chain. In other words, the top predator can invade the system.

In the region between the Hopf bifurcation curves H_3^+, $H_{3_2}^-$ and $H_{3_1}^-$ there is stable coexistence of bacteria, ciliates and carnivore (prey, predator and top predator).

A Bautin bifurcation point L_1 with zero first Lyapunov coefficient, separates the subcritical and supercritical Hopf bifurcations (see [13]). In this point a tangent bifurcation for limit cycles, $T_{c,3}$ originates, see Fig. 3. On the left side of L_1 there is a supercritical Hopf bifurcation and therefore below the curve $H_{3_2}^-$ there is a stable equilibrium and an unstable limit cycle. Close to L_1,

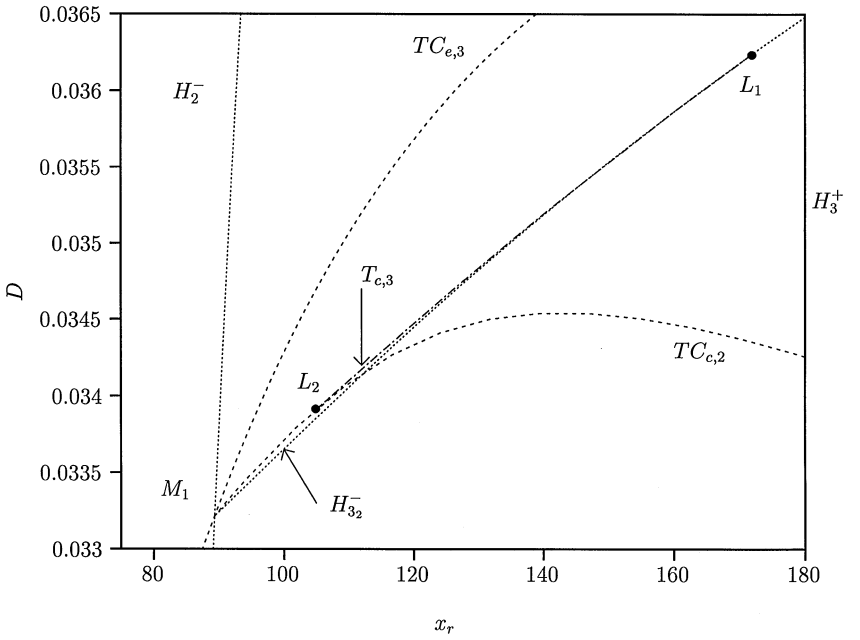

Fig. 3. Detail of the two-parameter bifurcation diagram Fig. 2. Dotted curves H_2^-, H_3^+ and $H_{3_2}^-$ mark Hopf bifurcations, curve $TC_{e,3}$ mark transcritical bifurcations, while $T_{c,3}$ marks a tangent bifurcation curve for positive limit cycles and curve $TC_{c,2}$ marks a transcritical bifurcation for limit cycles with $x_3 = 0$. Bautin bifurcation point L_1 is intersection point for bifurcation curves, $T_{c,3}$, H_3^+ and $H_{3_2}^-$. Point L_2 is intersection point for bifurcation curves, $T_{c,3}$ and $TC_{c,2}$

in the region between the curves $H_{3_2}^-$, $T_{c,3}$ and $TC_{c,2}$ there is one unstable equilibrium, one stable and one unstable limit cycle. The two limit cycles collapse and disappear at the tangent bifurcation for limit cycles, curve $T_{c,3}$.

The tangent bifurcation curve $T_{c,3}$ ends in point L_2 tangentially to the curve $TC_{c,2}$ where x_3 is zero. Close to L_2, in the region between the curves $H_{3_2}^-$ and $TC_{c,2}$ there is one unstable equilibrium and one stable limit cycle.

The supercritical Hopf bifurcation curves $H_{3_2}^-$, and H_2^- (with $x_3 = 0$), and the transcritical curves $TC_{e,3}$ and $TC_{c,2}$, intersect in a point denoted by M_1. Close to M_1, in the region between the curves $TC_{e,3}$ and $TC_{c,2}$ there is only one unstable equilibrium.

At point M_2 in Fig. 2 the tangent bifurcation curve $T_{e,3}$ intersects the transcritical bifurcation curve $TC_{e,3}$. Between these two curves there are two positive equilibria, while in the remaining region within the transcritical bifurcation curve $TC_{e,3}$ there is one positive equilibrium. In the region with two equilibria one is always unstable and the other is only stable in the region between the two Hopf bifurcation curves $H_{3_1}^-$, $H_{3_2}^-$ and H_3^+.

In the ecosystem model points M_2 and M_1 coincide. The dynamics in the neighbourhood of this point is discussed in [8, 14] in which the normal form in that point is studied. In the chemostat model these points are separated points.

The transcritical curve $TC_{e,3}$, Hopf bifurcation curves H_2^-, $H_{3_1}^-$, $H_{3_2}^-$ and H_3^+ and the tangent bifurcation curve $T_{e,3}$ given in Fig. 2 were already reported in [9, 11]. In the region between the curve $H_{3_1}^-$ and the curves F_{1_1} and F_{1_2}, which mark flip bifurcations or period doubling, there exists stable limit cycles. The dynamic behaviour of the limit cycles inside these flip bifurcations is studied in Sect. 4.1.

4 Limit cycles and chaotic attractors

4.1 Two-parameter bifurcation diagrams

The results given in the two-parameter bifurcation diagrams for limit cycles are based upon stability analysis of the limit cycles. Fig. 4 gives the bifurcation curves inside the region marked by the Hopf bifurcation curve $H_{3_1}^-$ where the positive equilibrium is unstable. A cascade of flip bifurcation curves leads to chaotic behaviour as the dilution rate D is increased at a constant concentration in the reservoir x_r. Only period-1 $\rightarrow$ 2 (F_{1_1}, F_{1_2} and F_{1_3}) and period-2 $\rightarrow$ 4 (F_{2_1}, and F_{2_2}) flip bifurcation curves are shown. The tangent bifurcation curves for the limit cycles, curves $T_{c,3_1}$, $T_{c,3_2}$, and $T_{c,3_3}$, are also shown. There is a cusp bifurcation for the tangent bifurcations for period-2 limit cycles, $T_{c,3_1}$. In order to study these phenomena in more detail we combine these results with those of one-parameter bifurcation diagrams in the next section.

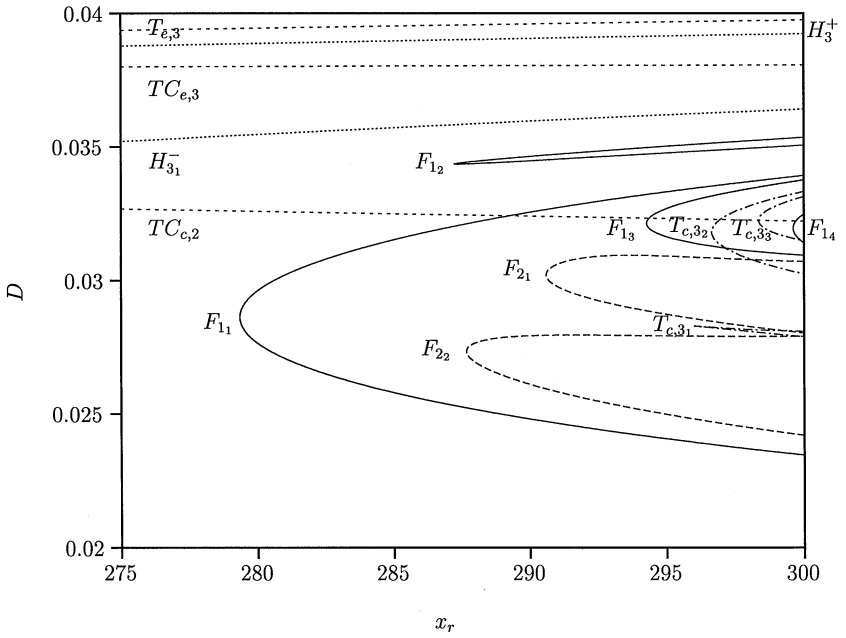

Fig. 4. Two-parameter bifurcation diagram for food chain with three population levels in chemostat situation (Eqs. 5, 6, 7, 8). Detail of Fig. 2. Dotted curves H_3^+, $H_{3_2}^-$ and $H_{3_1}^-$ mark Hopf bifurcations, curve $TC_{e,3}$ mark transcritical bifurcations while $T_{e,3}$ marks a tangent bifurcation curve and curve $TC_{c,2}$ marks a transcritical bifurcation for limit cycles with $x_3 = 0$. Curves F_{1_1}, F_{1_2} and F_{1_3} are period-1 $\rightarrow$ 2 flip bifurcation curves for limit cycles and F_{2_1} and F_{2_2} those of period-2 $\rightarrow$ 4. Curves $T_{c,3_1}$, $T_{c,3_2}$ and $T_{c,3_3}$ are tangent bifurcation curves

4.2 One-parameter bifurcation diagrams

In these one-parameter bifurcation diagrams for limit cycles and chaotic attractors peak (global and local) biomass of the top predator attained during a limit cycle or chaotic behaviour are shown as function of the control parameter D. Let us consider again the positive equilibrium values for the biomass of the carnivore, x_3, the positive equilibrium values as a function of the dilution rate D. In Fig. 5 we show these values for the carnivore biomass as a function of the dilution rate in the range $0.02 \leqq D \leqq 0.04\ \mathrm{h}^{-1}$, while the concentration in the reservoir is $x_r = 292.5\ \mathrm{mg\,dm}^{-3}$.

Above the one-parameter bifurcation diagram, the rotated two-parameter bifurcation diagram Fig. 4 is reproduced for the range $275\ \mathrm{mg\,dm}^{-3} \leqq x_r \leqq 292.5\ \mathrm{mg\,dm}^{-3}$. The region where the positive equilibrium is stable is indicated by the drawn line between the Hopf bifurcation curves H_3^+ and $H_{3_1}^-$ for the equilibrium with the largest biomass for the top predator x_3. The unstable equilibria (shown as dashed curves) are below the $H_{3_1}^-$ curve, between the curves $TC_{e,3}$ and $T_{e,3}$ and between the curves H_3^+ and $T_{e,3}$ for the equilibrium with the smallest biomass for the top predator x_3.

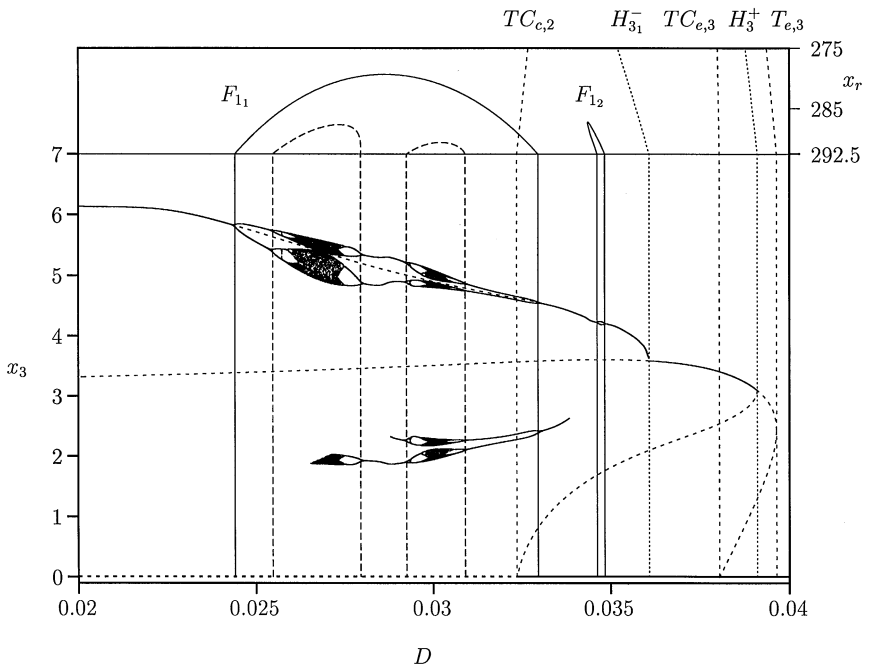

Fig. 5. One-parameter bifurcation diagram for peak (global and local) values of top predator as a function of dilution rate D, where concentration in reservoir is $x_r = 292.5$ mg dm^{-3}. Solid curves give stable equilibrium values and peak values of stable limit cycles. Dashed curves give unstable equilibrium values and (only global) peak values of unstable limit cycles. At the top the rotated two-parameter bifurcation diagram, Fig. 4, for $275 \leqq x_r \leqq 292.5$ is plotted. Bifurcation points (the D values for intersection points in two-parameter diagram (Fig. 4) of bifurcation curves with $x_r = 292.5$ line) are indicated by vertical lines

Starting from a point in phase space close to the latter equilibrium, the system converges asymptotically to the stable limit cycle with positive substrate, bacteria and ciliates while the carnivore population goes asymptotically extinct, that is $x_3 \to 0$ for $t \to \infty$. The intersection of these unstable equilibrium points with the $x_3 = 0$ axis gives the transcritical bifurcation, curve $TC_{e,3}$. The peak value of the dilution rate D for the curve with unstable equilibria marks the tangent bifurcation $T_{e,3}$. In a small interval between the curves $T_{e,3}$ and H_3^+ the equilibria with the largest x_3 are unstable too. In this case the system also converges asymptotically to a stable limit cycle with $x_3 = 0$, indicated by the horizontal line with $x_3 = 0$ for D values above the curve $TC_{c,2}$. An unstable limit cycle (only global peak values are shown as dashed curves) which originates from the subcritical Hopf bifurcation point H_3^+ is connected to the transcritical bifurcation $TC_{c,2}$ point. Below this curve we have stable limit cycles with $x_3 = 0$ and above this curve attractors with $x_3 > 0$. For D-values between the curves H_3^+, and $H_{3_1}^-$ the equilibria above this curve are stable; it is a point attractor. Below $H_{3_1}^-$ the system becomes

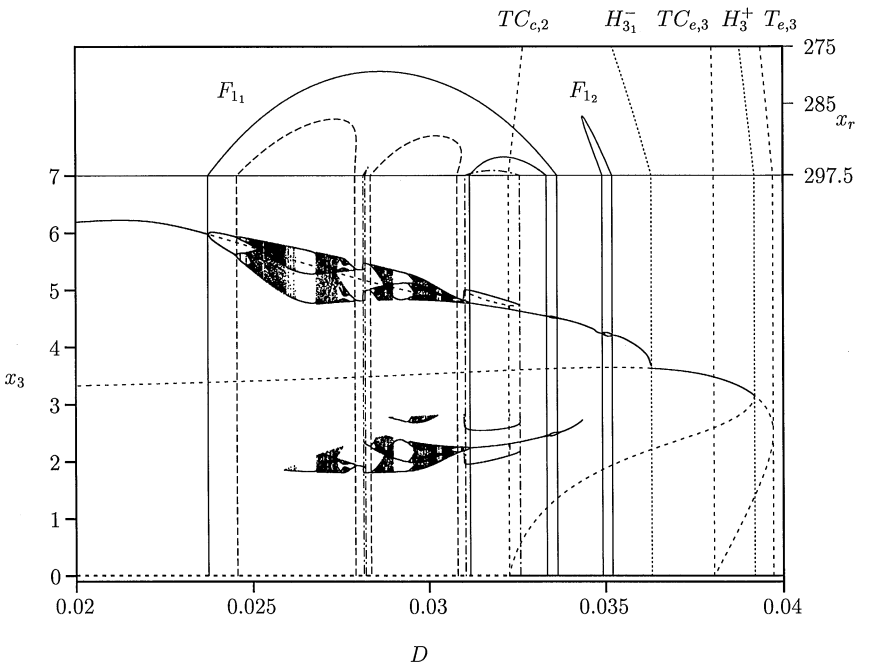

Fig. 6. One-parameter bifurcation diagram for peak (global and local) values of top predator as a function of dilution rate D, where concentration in reservoir is $x_r = 297.5$ mg dm^{-3}. See Fig. 5 for a description of the curves

unstable; starting from the perturbed equilibrium the system converges to a positive attractor, a limit cycle or chaotic attractor, until the D-values attains the value belonging to the second intersection point of the curve $H_{3_1}^-$ with the line $x_r = 292.5$ mg dm^{-3}. This point is not shown in Fig. 5 because it occurs for $D < 0.02$ h^{-1}.

The following procedure is used to obtain the results for the limit cycles and chaotic attractors in these diagrams. The system is integrated in time starting from a perturbed equilibria (the equilibrium value for the top predator was increased slightly). In case of multiple limit cycles or chaotic attractors, the system starts from the attractor for slightly different values of D in a continuation process. In order to get rid of the transients, integration is performed for a fixed time (we used 10 000 h) without examination of the results. From that point in time (until 15 000 h) the top predator peak value is shown as a dot in the diagram.

Period-1 $\rightarrow$ 2 (F_{1_1} and F_{1_2}) and period-2 $\rightarrow$ 4 (F_{2_1}, and F_{2_2}) flip bifurcation curves are shown in the diagram. A route of periodic doubling leads to chaotic behaviour within the two Period-2 $\rightarrow$ 4 (F_{2_1} and F_{2_2}) curves.

In Fig. 1 the phase portrait for dilution rate equal to $D = 0.03$ h^{-1} and $x_r = 292.5$ mg dm^{-3} is shown. It illustrates the chaotic attractor which traces the surface of a "teacup" as in models for ecosystems, see [4].

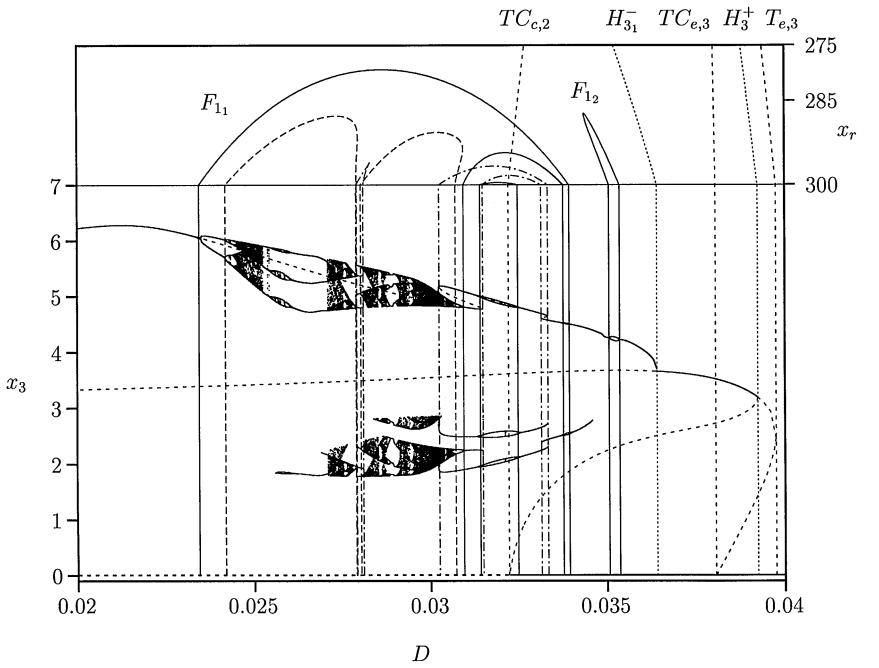

Fig. 7. One-parameter bifurcation diagram for peak (global and local) values of top predator as a function of dilution rate D, where concentration in reservoir is $x_r = 300$ mg dm^{-3}. See Fig. 5 for a description of the curves

The maxima for the biomass of the top predator in the chaotic region in Fig. 5 show that there is period-2 behaviour because the maxima fill two disjunct intervals. The trajectories lie on a Möbius band folded over the surface of the teacup, see also the white band in the centre of the attractor in Fig. 1.

We now discuss one-parameter bifurcation diagrams with higher concentration in the reservoir x_r, namely $x_r = 297.5$ mg dm^{-3} and $x_r = 300.0$ mg dm^{-3}, shown in Figs. 6 and 7, respectively. The dynamic behaviour for these values of x_r resembles that for $x_r = 292.5$ mg dm^{-3} but we will encounter new more complex dynamic phenomena.

For $x_r = 297.5$ mg dm^{-3}, when decreasing the dilution rate from the curve F_{1_1}, a period-2 limit cycles becomes a period-1 limit cycle again when the curve F_{1_3} is reached. Furthermore, three attractors coexist for certain values of the dilution rate, namely between the curves $T_{c,3_3}$ and $TC_{c,2}$. The initial values of the state variables determine to which limit cycle the system will evolve. For one of these coexisting limit cycles the top predator goes extinct in the long-term. The coexisting limit cycles were calculated using continuation with the parameter D. The end point values for the state variables of the preceding D-value were used as initial conditions. So, bounded by the tangent bifurcation $T_{c,3_2}$ there exists now a stable limit cycle which was not there with $x_r = 292.5$ mg dm^{-3}.

Comparison with Fig. 5 shows furthermore that the two disjunct intervals associated with the Möbius band collided. There is now a window with stable period-3 orbits. For $D = 0.029436\ \mathrm{h}^{-1}$, the right boundary of this window is formed by a flip bifurcation which introduces a cascade of periodic doubling. At the left boundary for $D = 0.02899\ \mathrm{h}^{-1}$ of this window the attractor widens abruptly to the full width of the chaotic region at the point of a tangent bifurcation for the period-3 limit cycle. The existence of such a window resembles those occurring in the well-known bifurcation diagram of the logistic map. Such a window is associated with a intermittency route to chaos, see for instance [26]. An unstable period-2 limit cycle (not shown in the figure) connects two tangent bifurcations for period-2 limit cycles $T_{c,3_1}$, close to the cusp bifurcation (see Fig. 4). This gives coexistence of two stable period-2 limit cycles in the region bounded by the tangent bifurcations $T_{c,3_1}$, $D \approx 0.028\ \mathrm{h}^{-1}$. A second window with period-3 orbits exists for $D \approx 0.0265\ \mathrm{h}^{-1}$.

For $x_r = 300\ \mathrm{mg\,dm}^{-3}$ the diagram given in Fig. 7 shows that one of the coexisting stable limit cycles in the region bounded by the tangent bifurcation curve $T_{c,3_2}$ for $x_r = 297.5\ \mathrm{mg\,dm}^{-3}$, disappeared in the region bounded by the tangent bifurcation curves $T_{c,3_3}$ (Fig. 4). The unstable limit cycle, shown in Fig. 6 cuts the stable limit cycle, and two curves representing unstable limit cycles connect now the tangent-bifurcations $T_{c,3_2}$ and $T_{c,3_3}$.

In the region bounded by the $T_{c,3_2}$ curves (Fig. 4) there is a period doubling for the remaining limit cycle denoted F_{1_4} (Fig. 4). For a small region of $D \approx 0.0303\ \mathrm{h}^{-1}$ there is also coexistence of a chaotic attractor and the stable limit cycle.

5 Biological implications

5.1 Effects of enrichment of the resources

We investigate the effects of enrichment of the resources on the stability of the food chain by the analysis of the bifurcation diagrams with increasing concentration of the resources in the feed, x_r, and a constant dilution rate, D. In [1, 2] the effects are analyzed on the mean abundances of the trophic levels for a food chain model with logistic prey; the ecosystem model.

The invasibility of the top predator is described in relation to the paradox of enrichment. With a bi-trophic food chain a stable limit cycle appears when the Hopf bifurcation H_2^- is passed by increasing the concentration in the reservoir x_r. This phenomenon is called the 'paradox of enrichment' [22]. With a tri-trophic food chain the situation is entirely different and much more complicated. From Fig. 2 we conclude that in the region between the curves H_2^-, $TC_{c,2}$ and $H_{3_1}^-$ the top predator stabilizes the system. There is a stable positive equilibrium for the tri-trophic food chain. The limit cycle of the bi-trophic food chain becomes unstable after the introduction of the top predator, i.e. the top predator invades the system. On the right side of the curve $H_{3_1}^-$, but still below the curve $TC_{c,2}$, this holds also true but now the

system converges to a positive limit cycle or a complex attractor instead of the limit point. Above the curve $TC_{c,2}$ the limit cycle of the bi-trophic food chain is stable, that is, top predators, if introduced in small numbers, are washed out again. Between the curves $TC_{c,2}$ and H_3^+ there is also at least one other attractor and the unstable limit cycle which originates from the subcritical Hopf bifurcation H_3^+ is the separator.

It is a regularly observed experimental fact that after some period of operation of a chemostat with a bi-trophic food chain, the dynamics changes notably; see [27]. It is stated that this is possibly due to 'mutation' of the prey to forms more resistant to predation, especially when the number of organisms is very low the population is sensitive to mutations. An alternative explanation is invasion of some top predator, which is possible for a large region of the control parameter space.

5.2 Influence of noise on dynamic behaviour

It is well-known that simple systems (discrete-time as well as continuous-time systems) can exhibit complex dynamics. In this paper we show that biologically more realistic models (they include maintenance and energy reserves) for a microbial food chain in the chemostat also can exhibit chaotic dynamics.

There is a controversy regarding the importance of chaos in population biology. For ecosystems, time-series analysis was used to show the possibility of chaotic dynamics of these systems, see for instance [28]. Food chains in chemostats are more tractable. The chemostat is an expermimental apparatus and a situation can be created such that some of the assumptions on which the model is based, are satisfied (for instance a homogeneous environment is obtained by stirring and the temperature is kept constant). This means that one does not have to rely on time-series analysis for the route to chaos can be studied experimentally like the way it is performed analytically.

Although the dynamics is determined in principle completely and precisely by the algorithm, that is the set of ODEs, in practice it is unpredictable due to numerical errors. The results presented are the solutions of a discrete-time scheme, which approximates the continuous-time evolution equations. Furthermore, the calculated solution of the discrete-time scheme is an approximation itself due to round-off errors. So, effectively the long-term future of a chaotic system is unpredictable because of the sentitivity upon initial conditions. This implies that with complex dynamic behaviour we have to focus on the shape of attractors and not to long-term time courses of the state variables.

Moreover, in reality there is always noise. First, there is *measurement* noise and this holds for the control parameters as well as the observed variables, i.e. the population biomass. In [15, 25] chaos is distinguised from measurement error in time series and this makes short-term predictions possible. In some regions of the bifurcation diagram, in Figs. 2 and 4, the dynamic behaviour depends very sensitively on the control parameters. The setting of

the control parameters, especially the dilution rate (assumed to be continuous but generally discontinuous in time), will be too inaccurate in practice. With respect to the observed variables, measurement noise associated with the use of a Coulter Counter for the measurement of the biovolumes, makes the different cycles with small differences in the amplitudes, as occuring with multiple solutions in Fig. 7, indistinguishable.

Second, some of the biological events at the individual level take place at random. This is called *dynamic* noise; see [24]. For organisms which propagate by binary fission the size at which they divide is stochastic, but also the parameters which determine the growth of an individual is subject to stochastic fluctuations which are much larger than errors due to round-off. This stochasticity is intrinsic and the 'law of large numbers limit' justifies the use of the deterministic model consisting of mean field equations.

Another random effect is associated with washout or predation. For the Holling type II functional response, which describes the predation, different mechanistic models are proposed in the literature, see for instance [11]. In these models two parameters, the handling time and the search time, are important. For low densities the hyperbolic relationship is not reasonable. In the *SEIR* epidemic model the linear functional response, that is the 'law of mass-action' holds. Also in that case the deterministic relationship fails for low numbers. In [20] it is replaced by a stochastic model and the influence on the chaotic behaviour is studied by numerical simulations.

Observe that contrary to the classical Lotka–Volterra model, the chemostat model with Holling type II functional response and maintenance included, system (5)–(8), does not predict unrealistic low numbers during oscillatory behaviour; see also Fig. 1. Furthermore we deal with microbial food chains, so the number of organisms is relatively large. This suggests that generally the mean field theory gives a good approximation.

Dynamic noise may destroy completely simple dynamics such as limit cycles; see for instance [23] where a one-dimensional map is iterated in the presence of noise, added multiplicatively. Because the bifurcation diagrams presented in Fig. 5 show a period doubling route to chaos similar to that of one-dimensional maps, we expect also destruction of simple dynamic behaviour with the introduction of noise in our model.

6 Discussion and conclusions

Autonomous microbial tri-trophic food chains under chemostat conditions were modelled here with a simplified version of the DEB model for each trophic level. For reasonable parameter values taken from literature, [3] and [18], a number of different attractors, stable equilibria, stable limit cycles and chaotic attractors occur.

It appears that the food chain introduces its own time-scale. At the individual level the parameter v_i which is proportional to the assimilation rate is a good measure for the time scale. For the population level it is the

expression $\mu_{i-1,i} - m_i$ representing the maximum attainable population growth rate. For a food chain which exhibits cyclic behaviour, the frequency imposes a new time-scale. For the set of parameter values used in this paper the cycle-period is very large, more than 300 h. This complicates experimental verification under laboratory conditions, as in chemostats. Furthermore, the band width of the chaotic oscillations is too small to distinguish it from measurement error.

Parts of the one-parameter diagrams, in which the peak (global and local) values of the top predator are given as a function of one control parameter, resemble the bifurcation diagram of one-dimensional quadratic maps such as the logistic map.

In some regions of the two-dimensional control parameter space, different competing attractor coexists and the initial point in the state space determines to which attractor the system will evolve. The attractors resemble those of ecosystem models in the literature, for instance the chaotic attractor traces the surface of a "teacup".

The information of one- and two-parameter bifurcation diagrams is presented in one diagram. This facilitates the analysis of the complex dynamic behaviour ranging from equilibria and limit cycles to chaotic behaviour via a rich set of local, and eventually global bifurcations, eventually including boundary crises. The combination of the results of continuation of bifurcation curves and long-term behaviour minimizes the overlook of relevant bifurcations.

Acknowledgements. The authors like to thank Hugo van den Berg and Yuri Kuznetsov for valuable discussions and Wim van der Steen for corrections in the text. The research of the second author was supported by the Netherlands Organization for Scientific Research (NWO).

References

1. P. A. Abrams and J. D. Roth. The effects of enrichment of three-species food chains with nonlinear functional responses. Ecology, **75**(4): 1118–1130, 1994
2. P. A. Abrams and J. D. Roth. The responses of unstable food chains to enrichment. Evolutionary Ecology, **8**: 150–171, 1994
3. A. Cunningham and R. M. Nisbet. Transients and oscillations in continuous culture. In M. J. Bazin, editor, Mathematical Methods in Microbiology, pp. 77–103, 1983
4. A. Hastings and T. Powell. Chaos in a three-species food chain. Ecology, **72**(3): 896–903, 1991
5. D. Herbert. Some principles of continuous culture. In G. Tunevall, editor, Recent progress in Microbiology, pp. 381–396, Oxford, England, 1958. Blackwell
6. A. I. Khibnik, Yu. A. Kuznetsov, V. V. Levitin and E. V. Nikolaevs. Continuation techniques and interactive software for bifurcation analysis of ODEs and iterated maps. Physica D, pp. 360–371, 1993
7. A. Klebanoff and A. Hastings. Chaos in one-predator, two-prey models: General results from bifurcation theory. Mathematical Biosciences, **122**: 221–233, 1994
8. A. Klebanoff and A. Hastings. Chaos in three-species food chain. J. Math. Biol., **32**: 427–451, 1994

9. B. W. Kooi and S. A. L. M. Kooijman. Existence and stability of microbiol prey-predator systems. J. theor Biol., **170**: 75–85, 1994
10. B. W. Kooi and S. A. L. M. Kooijman. The transient behaviour of food chains in chemostats. J. theor. Biol., **170**: 87–94, 1994
11. S. A. L. M. Kooijman. Dynamic Energy Budgets in Biological systems; Theory and Applications in Ecotoxicology. Cambridge University Press, 1993
12. M. Kot, G. S. Sayler, and T. W. Schultz. Complex dynamics in a model microbial system. Bull. Math. Biology, **54**: 619–648, 1992
13. Yu. A. Kuznetsov. Elements of Applied Bifurcation Theory, volume 112 of Applied Mathematical Sciences. Springer-Verlag, New York, 1995
14. Yu. A. Kuznetsov and S. Rinaldi. Remarks on food chain dynamics. Mathematical Biosciences, **124**(1): 1–33, 1996
15. R. M. May. Necessity and chance: deterministic chaos in ecology and evolution. Bull. of the American Mathematical Society, **32**(3): 291–308, 1995
16. K. McCann and P. Yodzis. Biological conditions for chaos in a tree-species food chain. Ecology, **75**(2): 561–564, 1994
17. J. Monod. Recherches sur la croissance bactériennes. Hermann, Paris, 1942
18. R. M. Nisbet, A. Cunningham and W. S. C. Gurney. Endogenous metabolism and the stability of microbial prey-predator systems. Biotechnol. Bioeng., 25: 301–306, 1983
19. S. Pavlou and I. G. Kevrekidis. Microbial predation in a periodically operated chemostat: A global study of the interaction between natural and externally imposed frequencies. Mathematical Biosciences, **108**: 1–55, 1992
20. D. A. Rand and H. B. Wilson. Chaotic stochasticity: a ubiquitous source of unpredictability in epidemics. Proc. R. Soc. Lond. B, **246**: 179–184, 1991
21. M. L. Rosenzweig. Paradox of enrichment: destabilization of exploitation ecosystems in ecological time. Science, **171**: 385–387, 1971
22. M. L. Rosenzweig and R. H. MacArthur. Graphical representation and stability conditions of predator-prey interactions. Amer. Natur., **97**: 209–223, 1963
23. W. M. Schaffer and M. Kot. Nearly one-dimensional dynamics in an epidemic. J. theor. Biol., **112**: 403–427, 1985
24. J. C. Schouten, F. Takens and C. M. van de Bleek. Estimation of the dimension of a noisy attractor. Physical Review E, **50**(3): 1851–1861, 1994
25. G. Sugihara and R. M. May. Nonlinear forecasting as a way of distinguishing chaos from measurement error in time series. Nature, **344**: 734–741, April 1990
26. J. M. T. Thompson and H. B. Stewart. Nonlinear Dynamics and Chaos. John-Wiley, 1986
27. H. M. Tsuchiya, J. F. Drake, J. L. Jost and A. G. Fredrickson. Predator-prey interactions of *Dictyostelium discoideum* and *Escherichia coli* in continuous culture. Journal of Bacteriology, **110**(3): 1147–1153, 1972
28. P. Turchin. Chaos and stability in rodent population dynamics: evidence from nonlinear time-series analysis. Oikos, **68**(1): 167–172, 1993